On Stability and Error Bounds of Describing Functions for Oscillatory Control of Movements

Artur M. Arsenio
Artificial Intelligence Lab
Massachusetts Institute of Technology
545 Technology Square, Cambridge, MA 02139, USA
email:arsenio@ai.mit.edu

Abstract

Biological neural circuits are often modeled by neural oscillators consisting of two mutually inhibiting neurons. These oscillators explore the natural dynamics of the body coupled to a dynamic system, to execute complex tasks, which resembles biological structures in animals. Controlling (non)linear multi-variable systems with multiple nonlinear oscillators results in very complex systems. Although algebraic equations are now available for tuning the oscillators to accomplish a complex task, based on quasi-linear approximations by describing functions, it is essential to infer stability characteristics of the solutions, as well as establish error bounds for the solutions due to the approximation. This paper suggests solutions for these problems, by presenting a method for estimating stability and bounds on the estimated parameter errors.

1 Introduction

The capability of entraining the frequency of the input signal or resonance modes of dynamical systems have been used for the control of robotic arms during the execution of different tasks. The neural oscillator analysed on this paper is the one proposed by Matsuoka [6] inspired on biological neural systems. These oscillators have entrainment properties with an external signal or system to which they are coupled over a large range of signal amplitudes and frequencies. They are also robust to disturbances.

There is biological evidence for the existence of oscillation pattern generators in animals, and humans often exploit the natural dynamics of the body to carry out tasks spending the minimum of energy. Through local adaptation, the neural oscillator cancels the damping of the coupled dynamical system and entrains its resonance frequency. In addition, multiple oscillators may be connected in networks to control Multiple-Input-Multiple-Output Systems (MIMO), so that complex behaviors may emerge [2].

However, neural oscillators depend on parameters that have to be tuned in order to achieve the desired performance [1]. The frequency and amplitude of oscillations of the different physical variables controlled depend on the value of these parameters. Therefore, it is essential a good understand of how to tune the parameters and on how small changes of these parameters will affect the performance of the neural oscillator, either to an input signal or when coupled with a dynamical system.

This paper addresses the estimation of stability properties and error bounds on the estimates, since parameter tuning, stability and error determination for MIMO systems connected to multiple neural oscillators is still lacking theoretical support. This analysis applies graphical tools, but data on the graphs are determined by algebraic equations, proposed in [1] for single oscillators and in [2] for multiple oscillators connected to multivariable systems. Since this method avoids simulation, it is not necessary the numerical integration of differential equations for building tables with parameter values.

Frequency domain methods may not be applied directly to nonlinear systems because frequency response functions cannot be defined for these systems. Driving the same linearity by inputs of different forms results in different linear approximations. These quasi-linear functions [5], [7], that describe approximately the transfer characteristics of the nonlinearity, are called describing functions (DF). The DF analysis results in small errors only if the linear element of the system has low-pass filter properties (thereafter called the filtering assumption). They are obtained by expanding the output signal in a Fourier series, and by neglecting harmonics different from the fundamental. Of course, this introduces errors on the estimates.

The Matsuoka neural oscillator consists of two neurons inhibiting each other mutually. Each neuron have two states variables, as illustrated in Figure 1. Thereafter, the nonlinearity n_{osc} and the describing function N will refer to the nonlinear dynamics for all the oscillator (unless stated otherwise), which follows the following equations:

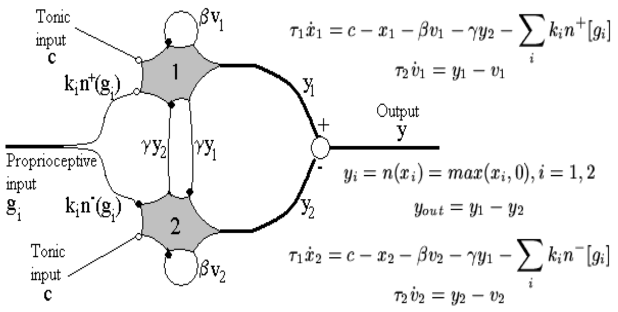

Figure 1: Dynamics of the Matsuoka neural oscillator, which is composed by two inhibiting neurons.

with parameters: c is a positive tonic input, τ_1 and τ_2 are positive time constants, β, γ and $k_i \geq 0$ are weights, and g_i is an external input to the oscillator. There are two types of nonlinearities: $n(u) = n^+(u) = max(u, 0)$, and $n^-(u) = -min(u, 0) = max(-u, 0)$, with u being the nonlinearity input. The problem of tuning oscillators consists on finding the set of parameters which result in desired amplitudes D and frequency of oscillation w (and phase-shifts phi, for MIMO systems). Or, for a given set of parameters, to find the oscillation characteristics w, D, and phi.

2 Stability

Lets first consider an analytical method to determine stability, described in [5] for a simple describing function, which approximates the overall oscillator as a nonlinear element. The first step in the error analysis is to check for *nondegeneracy*, i.e., nonzero degree relative to Ω, [3]. The conditions for a system to be stable are derived next. For a close-loop SISO system to oscillate it is necessary that $1 + N(D, w)G(jw) = 0$. Expressing this relation in terms of its real and imaginary parts, $U(D, w) + jV(D, w) = 0$.

Allow small perturbations in the limit cycle amplitude, rate of change of amplitude, and frequency, and introduce therefore,

$$D \rightarrow D + \Delta D, \quad w \rightarrow w + \Delta w + j\Delta\sigma$$

knowing that the perturbation in the rate of change of amplitude has been associated to the frequency term, so that $\Delta\sigma = -\dot{D}/D$. By substitution,

$$\frac{\partial U}{\partial D}\Delta D + \frac{\partial U}{\partial w}(\Delta w + j\Delta\sigma) + j\left(\frac{\partial V}{\partial D}\Delta D + \frac{\partial V}{\partial w}(\Delta w + j\Delta\sigma)\right) = 0$$

Solve for real and imaginary parts, eliminating Δw,

$$\left(\frac{\partial V}{\partial w}\frac{\partial U}{\partial D} - \frac{\partial U}{\partial w}\frac{\partial V}{\partial D}\right)\Delta D = \left[\left(\frac{\partial U}{\partial w}\right)^2 + \left(\frac{\partial V}{\partial w}\right)^2\right]\Delta\sigma. \quad (1)$$

For a stable limit cycle, $\frac{\Delta D}{\Delta\sigma} > 0$, and therefore

$$\frac{\partial V}{\partial w}\frac{\partial U}{\partial D} - \frac{\partial U}{\partial w}\frac{\partial V}{\partial D} > 0. \quad (2)$$

From (2), the degree is given by

$$d\left(1 + NGorN + \frac{1}{G}or1/N + G, \Omega, 0\right) = \sum_i sgn(detJ_i) \quad (3)$$

where the summation is over all DF solutions in Ω, and J_i is given by
$J_i = \left[\begin{array}{cc} \frac{\partial U}{\partial w} & \frac{\partial U}{\partial d_1} \end{array} ; \begin{array}{cc} \frac{\partial V}{\partial w} & \frac{\partial V}{\partial d_1} \end{array}\right]$.

Example 1 Consider the 2^{th} order system,

$$\Theta(jw) = G(jw)Y(jw) = \frac{k}{k - mw^2 + bwj}Y(jw) \quad (4)$$

Using the algebraic equations determined in [1], [2], it is very fast and straightforward to plot a graph as illustrated in Figure 2. It should be stressed here that the graph is build using analytical equations, and not simulation results. This way, stability properties may be inferred with high precision, because the equations may be solved for as many values as the desired. As easily seen in Figure 2, at the intersection with the origin, equation (2) is satisfied, because

$$\partial V/\partial w > 0, \partial U/\partial w > 0, \partial U/\partial D > 0 \; and \; \partial V/\partial D < 0.$$

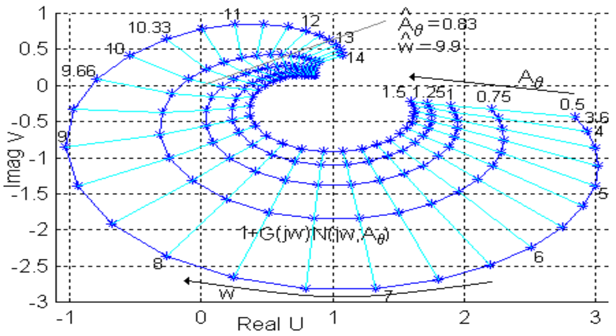

Figure 2: Graph of 1+N(D,jw)L(jw) in the complex plane. After drawing for different amplitude and frequency values, the intersection with the origin defines the frequency and amplitude of oscillation. This graph is very useful to infer stability. Parameters: $k = 30$, $m = 0.4$, $b = 2$. Oscillator parameters, for all the results in the paper: $\beta = \gamma = 2$, $\tau_1 = 0.1$, $\tau_2 = 0.2$, $c = 1$.

Stability may also be demonstrated by decomposing the system $1 + N(D, jw)G(jw) = 0 \longrightarrow 1/G(jw) + N(D, jw) = 0$. Thus, for $\hat{w} = 9.9$, $U = N_u + (1/G)_u$, and $V = N_v + (1/G)_v$ (a plot of N is shown ahead in Figure 6), the same result as before is obtained, i.e., the limit cycle is stable.

$$\frac{\partial(1/G)_u}{\partial w} = -2mw/k = -0.26 < 0, \frac{\partial N_u}{\partial w} < 0, \frac{\partial N_u}{\partial D} \approx 0$$
$$\frac{\partial(1/G)_v}{\partial w} = b/k = 0.067 > 0, \frac{\partial N_v}{\partial w} \approx 0, \frac{\partial N_v}{\partial D} > 0.$$

Stability analysis can also be evaluated using the limit cycle criterion [7], (the proof can be found in [5]):

Limit Cycle Criterion: *Each intersection point of the curve of the stable linear system G(jw) and the curve and the curve -1/N(D) corresponds to a limit cycle. If points near the intersection and along the increasing-D side of the curve -1/N(D) are not encircled by the curve G(jw), then the corresponding limit cycle is stable. Otherwise, the limit cycle is unstable.*

The intersection of both plots at the same frequency determines the frequency and amplitude of oscillations for the limit cycle, as shown in Figure 3.

Example 2 Lets analyse the case of one oscillator ($y_2 = 0$) connected to the following 4^{th} order system:

$$\begin{aligned} m_1\ddot{\theta}_1 + c_1\dot{\theta}_1 + (k_1 + k_T)\theta_1 - k_T\theta_2 &= k_1 y_1 \\ m_2\ddot{\theta}_2 + c_2\dot{\theta}_2 + (k_2 + k_T)\theta_2 - k_T\theta_1 &= k_2 y_2 \end{aligned} \quad (5)$$

The transfer matrix G results from applying the Fourier transform. The Nyquist criterion for a system to oscillate is

$$|I + N_{osc}(D, jw)G(jw)| = 0 \quad (6)$$

where $N_{osc_1} = N\Lambda$, $\Lambda_{11} = 1$, and the other elements of Λ are zero. This is equivalent to $|1+N(D, jw)G_{11}| = 0 \iff |1/N(D, jw) + G_{11}| = 0$, and thus it is possible to build the graph in Figure 3, and check stability through the limit cycle criterion.

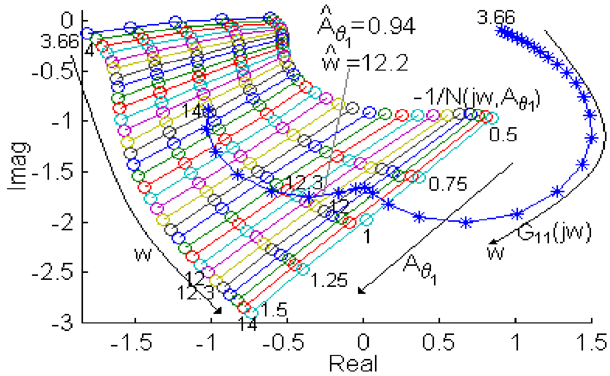

Figure 3: Graphs of -1/N(D,jw) and $G_{11}(jw)$ in the complex plane. Parameters used: $m_i = 1$, $c_i = 3$, $k_i = 100$, for i=1,2, and $k_T = 30$. The estimated oscillation frequency is $\hat{w} = 12.2$, with amplitude $\hat{D} = \hat{A}_{\theta_1} = 0.94$. After drawing -1/N(D,jw) for different amplitude and frequency values, and $G_{11}(jw)$ for different frequency values, the intersection of both curves at the same frequency corresponds to the frequency and amplitude of oscillation, and the limit cycle is stable.

As before, stability may also be inferred by application of condition (2), being $U = (1/N)_u + G_{11_u}$ and $V = (1/N)_v + G_{11_v}$ obtained directly from Figure 3, resulting:

$$\frac{\partial(\frac{1}{N})_u}{\partial w}, \frac{\partial G_{11_u}}{\partial w} < 0, \frac{\partial(\frac{1}{N})_v}{\partial w}, \frac{\partial(\frac{1}{N})_u}{\partial D}, \frac{\partial(\frac{1}{N})_v}{\partial D} > 0, \frac{\partial G_{11_v}}{\partial w} \approx 0.$$

2.1 Multiple Oscillators

Lets now extend the previous analysis to MIMO systems connected to multiple neural oscillators. For a system to present oscillations, the Nyquist criterion for MIMO systems requires that $|G^{cl}| = 0$ (from equation (6)), [8]. However, the oscillator dynamics is nonlinear, and the plant may or may not be linear. Thus, the transfer matrix is not independent of the n amplitudes of oscillation, and therefore $n-1$ more constraint are required for oscillations, which are applied to the $n-1$ rows of G^{cl} (all rows could be used, instead of the determinant, since the determinant constraint introduces a singularity in the matrix, [2]):

$$G^{cl}_{i,1} D_{\theta_1} + \sum_{k=2}^{n-1} G^{cl}_{i,k} D_{\theta_k}(cos(\varphi_k) + j sin(\varphi_k)) = 0 \quad (7)$$

Expressing (6) and (7) in terms of its complex parts, results $\sum_{i=1}^{n} U_i + jV_i = 0$. Allow small perturbations in the limit cycle rates of change of amplitude, amplitude ($D_i \to D_i + \Delta D_i$), phase-shift ($\varphi_i \to \varphi_i + \Delta\varphi_i + i\sum_{j=1}^{n} \Delta\sigma_{D_j}$) and frequency ($w \to w + \Delta w + i\sum_{j=1}^{n} \Delta\sigma_{D_j}$). Therefore, $2n$ equations are available, for both complex parts to cancel. The frequency w is unknown, there are n unknowns for the variation in amplitudes ΔD_i, $n-1$ unknowns for the phase-shift variation $\Delta\varphi_i$, $i > 1$ between the first and the i^{th} outputs, and n for the rate of change σ_{D_j}, in a total of $3n$ unknowns. Similarly to the previous section, n constraint are used to eliminate the frequency w and the phase-shifts from the remaining n equations. These equations are then combined to define a transformation $J = M^{-1}N$, described by (8). For a locally stable limit cycle, J must be positive definite.

$$\left[\Delta\sigma_{D_1} \ldots \Delta\sigma_{D_n}\right]^T = J_{n\times n}[\Delta D_1 \ldots \Delta D_n]^T \quad (8)$$

Example 3 Lets analyse the stability of two oscillators connected to a 4^{th} order system described by (5). In Figure 4-a it is plotted the graph corresponding to $|L(jw) + 1/N(D_1, D_2, jw)| = U_1 + iV_1$, where $N(D_1, D_2, jw) = [N^1(N(D_1, jw)\ 0; 0\ N^2(N(D_2, jw)]$ and N^i is the describing function of each oscillator, [1]. The intersection with the origin occurs for two frequencies, $w_1 = 8.5$ and $w_2 = 10.8$, corresponding to two different limit modes of oscillation (on phase and in phase opposition, respectively). Since this condition is not enough to infer stability, there are several values of (D_1, D_2) which cancel the determinant at these frequencies. However, the second condition given by (7) is used to impose additional constraints.

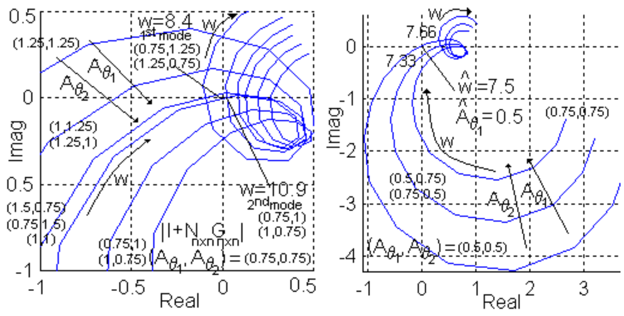

a) b)

Figure 4: a) Graph for system with two stable oscillation modes, where $k_1 = k_2 = 50$, and $k_T = 30$. b) Graph for system with one stable limit cycle, where $k_1 = k_2 = 25$, and $k_T = 60$.

The same reasoning applies for the system in Figure 4-b. However, for the parameters selected there are now no intersection with the origin for the 2^{th} resonance mode (high frequency mode). Despite the low resolution data in the figure, small amplitude values will not cause high frequency oscillations, because the oscillators do not entrain this plant natural mode for small input amplitudes.

3 Error Bounds

Being DFs an approximate method, it is crucial an error analysis of the describing functions, to check for error bounds. The goal of this analysis is to find a set Ω of frequencies and amplitudes within which the true values are contained. A detailed analysis for single input single output (SISO) systems with simple nonlinear elements is presented in [3]. However, the nonlinearity represented by the overall dynamics of the neural oscillator is very complex.

For a π-symmetric signal $x(wt + 2\pi) = -x(t)$ with period $2\pi/w$, define $K = \{0, 1, 3, 5, \cdots\}$ and $K^* = \{3, 5, \cdots\}$. Thus,

$$x = imag\left(\sum_{k\in K} d_k e^{jkwt}\right), \quad x^* = imag\left(\sum_{k\in K^*} d_k e^{jkwt}\right)$$

where $d_1 = D$, and x^* is the part of the solution neglected by the estimate of the DF. The estimate is reliable only if x^* is small. Since the filtering assumption is the requirement for a small x^*, the performance of the linear part of the system in filtering unwanted harmonics is given by:

$$\rho(w) = \sqrt{\sum_{k\in K^*} |G(jkw)|^2} \qquad (9)$$

The function used to find the DF output error is

$$p(D) = \sqrt{||n(Dsin(wt))||_2^2 - |DN_d|^2} \qquad (10)$$

where n is the nonlinearity (accounting for the dynamics of all the oscillator), N_d the describing function of the nonlinearity, and $||\cdot||_2$ is the L_2 norm on $[0, 2\pi/w]$. The function p may be replaced by an upper bound αD if n has finite gain α, $|n(x)| \leq \alpha|x|$, with some loss of accuracy in the eventual error estimate. For the neural oscillator, N_d was computed from the solutions of the algebraic equations, [1], and then $p(D)$ was determined using *Matlab*.

The function that measures the error introduced by neglecting higher harmonics at the input of n is given by (where $||\cdot||_\infty$ is the L_∞ norm), [3],

$$q(D,\epsilon) = sup_{||x^*||_\infty \leq \epsilon} ||n(Dsin(wt) + x^*) - n(Dsin(wt))||_2.$$

The smaller the value of q, the better the eventual error estimate. An upper bound was used on this paper for q. As described in [3], one has to find an upper bound on the higher harmonic error $\epsilon > 0$, and then finding the set Ω. Inequality (11) has to be satisfied,

$$\rho(w) min\{q(D,\epsilon) + p(D), r(D,\epsilon)\} \leq \epsilon \qquad (11)$$

where $r(D,\epsilon) = \sqrt{2} sup_{|y_1| \leq d_1 + \epsilon} |n(y)|$. A closed-bounded set Ω, which contains $(\hat{w}, \hat{D})$ - the estimated frequency and system output amplitude, is found by all points in the neighborhood that satisfy

$$\eta = \left| N(D) + \frac{1}{G(jw)} \right| / \sigma(w, D) \leq 1 \qquad (12)$$

where $\sigma(w, D) = q(D, \epsilon(w, D))/D$. The tightest bounds correspond to small values of ϵ. There are several ways for finding Ω, as described in [3]. One can surround $(\hat{w}, \hat{D})$ by a grid of points, find ϵ at each point and calculate the ratio η. The boundary of Ω is given by the points corresponding to a unit ratio. A method that improves the accuracy of the results is poleshifting, [3]. Only two equations have to be changed, by adding an extra term:

$$\tilde{q} = \sup_{||x^*||_\infty \leq \epsilon} ||\ n(Dsin(wt) + x^*) - n(Dsin(wt)) - \phi x^*\ ||_2$$
$$\tilde{\rho}(w, \phi) = \sum_{k\in K^*} \left| \frac{G(jkw)}{1 + \phi G(jkw)} \right|^2$$

It is now possible to choose ϕ to minimize $\tilde{\epsilon}$. The poleshift factor ϕ is arbitrary. One can determine the optimal value through an optimization process for the best bounds, or through a worst-case analysis, by selecting $\phi = 0$ (value used for the experiments in this section), or even $\phi = 1/2(\alpha_1 + \alpha_2)$, if the nonlinearity has slope bounds α_i.

Example 4 Lets determine the error bounds for the systems in examples 1 and 2. As shown in Figure 5-a, the measured values for the frequency of oscillation are $w = 9.88$ and for the oscillator input amplitude $D = 0.85$, and the predicted ones $\hat{w} = 9.9$ and

$\hat{D} = 0.83$, with $\Omega = \{w \in [9.6, 10.2], D \in [0.75, 1]\}$. Note that the discretization of D is very small (scale is 0.25), and thus a higher resolution for D would improve the error bounds, making other curves crossing the unity, giving a more precise boundary. Figure 5-b shows the error bounds for the system introduced in example 2, which are $\Omega = \{w \in [11.4, 13], D \in [0.75, 1.0]\}$.

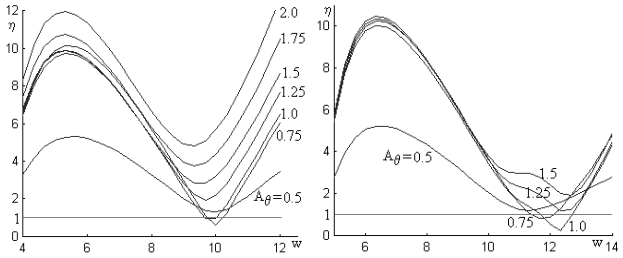

a) b)

Figure 5: Estimation of Ω using a grid of points, and checking intersection with unity, for a) $w = 10$, and b) $w = 12.9$.

Another way of checking error bounds is through the use of error discs, [3]. For which frequency, draw a disc of radius σ, and draw circles on the $-1/G$ locus as in Figures 6 and 7. The points where the tangent of the circles intersect the $N(D, w)$ locus at the same frequency give the range for w and D.

Example 5 The graphical method for error bounds based in the use of error discs is shown in Figures 6 and 7. This method allows to visualize the variation of the uncertainty with frequency.

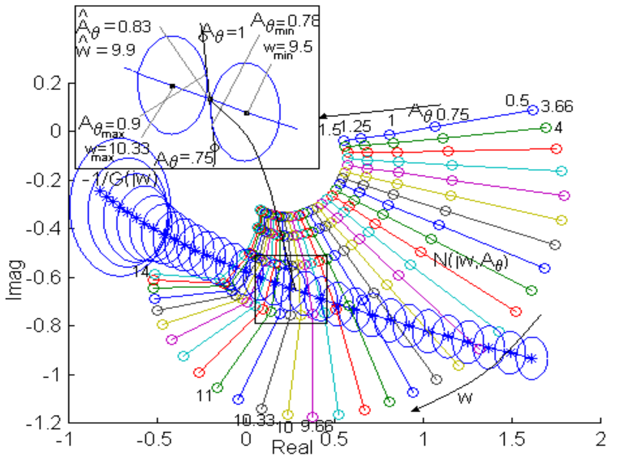

Figure 6: Error bounds for coupled system with $w_n = 8.66$. The error bounds in frequency and amplitude are $\Omega = \{w = [9.6, 10.2], D = [0.78, 0.9]\}$, being the estimated values $\hat{w} = 9.9$ and $\hat{D} = 0.83$. The real values are $w = 9.88$ and $D = 0.85$.

The degree given by (3) can also be determined by

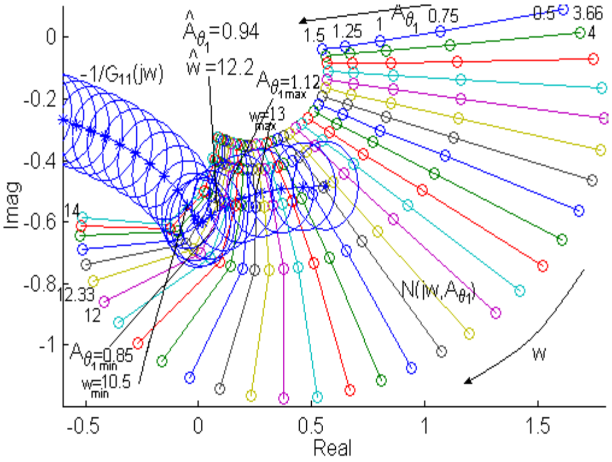

Figure 7: Error bounds for coupled system with $w_n = 12.24$. The error bounds in frequency and amplitude are $\Omega = \{w = [10.5, 13], D = [0.85, 1.12]\}$, being the estimated values $\hat{w} = 12.2$ and $\hat{D} = 0.94$. The real values are $w = 12.9$ and $D = 1$.

inspection. Considering the $-1/G$ loci as a spring, and put pegs at the points correspondent to w_{min}, w_{max}, D_{min} and D_{max}. Now pull the string from the pegs. The degree is nonzero if the strings still cross, otherwise the degree is zero and the analysis has failed, [3].

4 Extension to Multivariable Systems

Elements of the transfer matrices for MIMO systems are complex transfer functions. Singular value decomposition (SVD) [8] provides the tools for a notion of the *size* of $\underset{\sim}{G}(jw)$ versus frequency, equivalent to a MIMO gain. The singular values of a complex matrix $\underset{\sim}{G}(jw)$ are given by (being λ the eigenvalues):

$$\sigma_i^2(\underset{\sim}{G}) = \lambda_i\left(\underset{\sim}{G}^H\underset{\sim}{G}\right) = \lambda_i\left(\underset{\sim}{G}\underset{\sim}{G}^H\right) > 0, \tag{13}$$

for i=1,... k, being k the rank of $\underset{\sim}{G}(jw)$ and $\underset{\sim}{G}(jw)^H$ the complex conjugate transpose of $\underset{\sim}{G}(jw)$. The singular value decomposition is given by [8]:

$$\underset{\sim}{G} = \underset{\sim}{U}\Sigma\underset{\sim}{V}^H, \quad \Sigma = \underset{\sim}{U}^H\underset{\sim}{G}\underset{\sim}{V} \tag{14}$$

where Σ is a diagonal matrix, which elements are the singular values of $\underset{\sim}{G}$, and the columns of U and V the left/right singular vectors of $\underset{\sim}{G}$. Direction information can also be extracted from the SVD. Indeed, for inputs along U_i, the outputs along V_i will be amplified by a gain σ_i. Thus, σ_{max} of $\underset{\sim}{G}(jw)$ define maximum amplification of a unit sinusoidal input at frequency w, and the corresponding singular vector the direction for maximum amplification. One useful norm for such stable systems is the H_∞ norm, defined by

$$||\underset{\sim}{G}||_\infty = sup_w \sigma_{max}\left[\underset{\sim}{G}(jw)\right] \tag{15}$$

For the derivation of the inequalities, consider $X = X_1 + X^*$ as the input vector for the oscillators, $X = -Gn(X)$, and that $X^* = P^*X$ contains only harmonics whose indexes are in K^*. Thus,

$$X^* = -G(jw)P^*n(X_1 + X^*) \tag{16}$$

$$X_1 = -G(jw)P_1n(X_1 + X^*) \tag{17}$$

where n is a column vector whose elements are the dynamics of each neural oscillator. Writing (16) as $X^* = F(w, D_1, X^*)$, it will be necessary to find an inequality that guarantees $||X^*||_2 \leq \epsilon \Rightarrow ||F||_2 \leq \epsilon$, in such a way that F maps $B(0, \epsilon)$ to itself, using the L_2 norm for vectors. Thus,

$$F(w, D_1, X^*) = -Imag\left(\sum_{k\in K^*} G(jkw)c_k e^{j(kwt+\varphi_k)}\right)$$

for $n(D_1 sin(wt) + X^*) = Imag\left(\sum_{k\in K} c_k e^{j(kwt+\varphi_k)}\right)$. By application of Schwartz's inequality,

$$||F||_2^2 \leq \left[\sum_{k\in K^*} \sigma_{max}^2(G(jkw)\right] \sum_{k\in K^*} ||c_k||_2^2 = \rho^2||P^*n||_2^2 \tag{18}$$

For the results presented in this paper, the maximum amplification of unwanted harmonics not filtered by the linear part of the system is given by:

$$\rho(w) = \sqrt{\sum_{k\in K^*} \sigma_{max}^2[G(jkw)]} \tag{19}$$

This corresponds to a worst case analysis, and therefore it is independent of D_i and φ_i. The computation of $\rho(w)$ requires only a finite number of terms if G is a stable strictly proper transfer matrix. From (17) and (20) results the phasor equation (22),

$$-E(D_1, X^*)D_1 sin(wt) = P_1\left[N(X_1 + X^*) - N(X_1)\right] \tag{20}$$

$$D_1 = G(jw)E(D_1, X^*)D_1 - G(jw)N(D_1)D_1 \tag{21}$$

where $D_1 = [d_{x1}\, d_{x2}e^{j\varphi_2} \cdots d_{xn}e^{j\varphi_n}]^T$, and N is a diagonal matrix which elements are the DFs of each neural oscillator. For an invertible matrix G results

$$\left[G^{-1}(jw) + N(D_1) - E(D_1, X^*)\right] D_1 = \underline{0}. \tag{22}$$

To estimate the bound lets consider the Schwartz Inequality

$$||P^*n(X)||_2^2 \leq ||P^*(n(X) - n(X_1))||_2^2 + \| P^*n(X_1) \|_2^2$$

so that the DF output error is

$$p(D_1) = \| P^*n(X_1) \|_2^2 = ||n(D_1 sin(wt)||_2^2 - ||D_1N(D_1)||_2^2.$$

This last relation results from the Pythagorean equality on the Hilbert space of square-integrable periodic functions. From (18), one obtains the inequality (23):

$$||F||_2 \leq \rho(w)(q(D_1, \epsilon) + p(D_1)) \leq \epsilon \tag{23}$$

The function that measures the error at the output of n is given by

$$q = sup_{||X^*||_2\leq\epsilon}||n(D_1 sin(wt) + X^*(t)) - n(D_1 sin(wt))||_2.$$

Finally, the resulting condition, using (22), is

$$\eta = ||[G^{-1} + N(D_1)]D_1||_2/q(D_1, \epsilon) \leq 1 \tag{24}$$

where ϵ is determined using (23), and $q(D_1, \epsilon) = ||E(D_1, X^*)D_1||_2$. A closed-bounded set Ω, which contains the estimated frequency, system output amplitudes and phase-shifts - $(\hat{w}, \sum_{i=1}^n \hat{D}_i, \sum_{i=2}^n \hat{\varphi}_i)$, is found by all points in the neighborhood that satisfy the inequality (24). A better bound could be achieved through pole shifting, similarly to the SISO case.

Of course, other norms could be used for $\rho(w)$ in equation (19), such as the H_∞ norm, given by (15). This norm would be conservative for some cases, but not when equal to $\sigma_{max}(G(jkw)$, for any k. This would be equivalent to $||F||_2/\epsilon = \gamma \leq 1$, where γ is the L_2 gain of ΔL, with $\Delta = P^*n(X)$ and $L = \sum_{k\in K^*} G(jkw)$ (which could be represented as an interconnection diagram for the error dynamics, [8]). In addition, the L_∞ norm could be used instead of the L_2 norm to find the error bounds.

The singular value decomposition may also be very useful in other situations, such as the analysis of neural oscillators inter-connected in networks. Indeed, when a neural oscillator has more than one input (from other oscillators or from other plant state-variables), it is often difficult to infer which connections should be made to get a desired performance. Thus, inputs which drive the system along the direction of a minimum singular will have a small effect in driving the plant, and may even be negligible for very small σ_{min}. On the other hand, the direction associated to σ_{max} is useful to not only infer maximum propagated errors, but also to determine the optimal inter-connection of networks, so that the network outputs will drive the system with the maximum amplitude, along the maximum singular direction.

For the results thereafter presented the neural oscillators are connected to a MIMO system with transfer matrix G, without mutual connections among the oscillators, i.e., the oscillators are coupled through the dynamics of the MIMO system (N, the approximated transfer matrix for the neural oscillators is diagonal, containing each element the approximated dynamics of each neural oscillator). If there were mutual connections, the computation of the error bounds p and q would be harder. In addition, it is assumed that all neural oscillators oscillate at only one resonance mode, [2] (indeed, a large spectrum of frequencies would imply the use of a Describing Function Matrix, [5]).

Example 6 For the system in Figure 4 of example 3, Figure 8 shows the graphs obtained from (24) varying D_1, D_2, φ and W. As shown, there are two resonance modes at $w = 8.6$ and at $w = 10.9$ with a well defined error interval of frequencies at $[8.3, 9]$ and $[10.2, 11.2]$. Figure 8-b shows the plot for the system in Figure 4-b of example 3. The system does not oscillate at the second resonance mode, and therefore the error intervals are only determined for the first mode, i.e., $w \in [7, 8]$, with $\hat{w} = 7.5$.

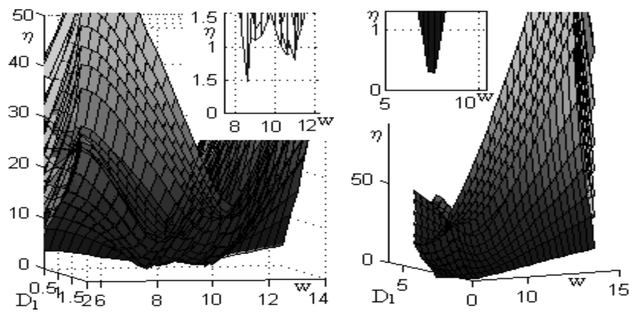

a) b)

Figure 8: Error estimation for a MIMO system for the parameters in example 3. Plots for one of the necessary conditions a) $k_1 = k_2 = 50$, and $k_T = 30$. b) $k_1 = k_2 = 25$, and $k_T = 60$.

The graphic method of error discs (example 5) might also be extended to two oscillators connected to a MIMO system. However, instead of error discs, the method would now consist of error spheres, and, for higher dimensions, hyperspheres.

5 Discussion and Conclusions

A method was presented to infer limit cycle stability and error bounds on the estimates introduced by using describing functions. For neural oscillators connected to a low-pass system, the higher harmonics of the signal are removed and the estimate is accurate, and therefore the intervals of uncertainty are small. Stability of multiple oscillators connected to a MIMO system was also analysed.

The work here presented is part of the humanoid robot project *Cog*, [4], shown in Figure 9-b. This analysis provides theoretical support to existing algorithms for the control of the robot arms using several biologically inspired Matsuoka neural oscillators (exemplified in Figure 9-a).

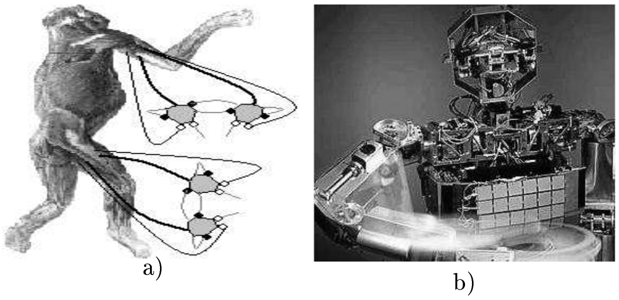

a) b)

Figure 9: a) Neural oscillators for the control of the motor system. b) Cog, a humanoid robot with two 6 DOF arms

The error bounds determined for the estimated parameters correspond to the expectations. Furthermore, the algebraic equations (which were applied for parameter tuning) are solved rapidly, so that building a graph to check stability is simple and fast.

A method was presented to estimate the multivariable error, which takes into account the maximum amplification of the error by the plant. Using this technique, error bounds are estimated for MIMO systems connected to multiple oscillators. SVD is also useful to check for the number/type of connections necessary in a network of multiple neural oscillators to achieve a desired performance.

Acknowledgments

The author was supported by a Portuguese government grant PRAXIS XXI BD/15851/98. Support for this research is provided by DARPA/ITO, contract number DABT 63-99-1-0012 for *Natural Tasking of Robots Based on Human Interaction Cues.*

References

[1] A. M. Arsenio, "Tuning of Neural Oscillators for the Design of Rhythmic Motions", accepted to IEEE Conf. on Robotics and Automation, 2000.

[2] A. M. Arsenio, "Neural Oscillator Networks for Rhythmic Control of Animats", submitted to From Animals to Animats 2000.

[3] A. R. Bergen, L. O. Chua, A. I. Mees and E. W. Szeto, "Error Bounds for General Describing Function Problems", IEEE Trans on Circuits and systems, 6 (29), June 82.

[4] R. A. Brooks, C. Breazeal, R. Irie, C. Kemp, M. Marjanovic, B. Scassellat and M. Williamson, "Alternate Essences of Intelligence", AAAI-98

[5] A. Gelb and W. Vander velde, "Multiple-Input Describing Functions and Nonlinear System Design", McGraw-Hill, 68.

[6] K. Matsuoka, "Sustained Oscillations Generated by Mutually Inhibiting Neurons with Adaptation", Biological Cybernetics, 52:367-376, 85.

[7] J-J. E. Slotine and W. Li, "Applied Nonlinear Control", Englewood Cliffs, Prentice-Hall, 91.

[8] K. Zhou and J. C. Doyle, "Essentials of Robust Control".